UCRL-16657 Rev.

University of California

Ernest O. Lawrence Radiation Laboratory

EFFECTS OF LOW TEMPERATURE AGING ON THE RESISTIVE TRANSITION OF SUPERCONDUCTING 70Zr-30Nb (Cb) IN PULSED MAGNETIC FIELDS

TWO-WEEK LOAN COPY

This is a Library Circulating Copy which may be borrowed for two weeks. For a personal retention copy, call Tech. Info. Division, Ext. 5545

DISCLAIMER

This document was prepared as an account of work sponsored by the United States Government. While this document is believed to contain correct information, neither the United States Government nor any agency thereof, nor the Regents of the University of California, nor any of their employees, makes any warranty, express or implied, or assumes any legal responsibility for the accuracy, completeness, or usefulness of any information, apparatus, product, or process disclosed, or represents that its use would not infringe privately owned rights. Reference herein to any specific commercial product, process, or service by its trade name, trademark, manufacturer, or otherwise, does not necessarily constitute or imply its endorsement, recommendation, or favoring by the United States Government or any agency thereof, or the Regents of the University of California. The views and opinions of authors expressed herein do not necessarily state or reflect those of the United States Government or any agency thereof or the Regents of the University of California.

Submitted to: Transactions
of the Metallurgical Society
of AIME

UCRL-16657 Rev.
Preprint

UNIVERSITY OF CALIFORNIA

Lawrence Radiation Laboratory
Berkeley, California

AEC Contrast No. W-7405-eng-48

EFFECTS OF LOW-TEMPERATURE AGING ON THE RESISTIVE TRANSITION OF SUPERCONDUCTING 70Zr-30Nb (Cb) IN PULSED MAGNETIC FIELDS

M. Suenaga, J. L. O'Brien, V. F. Zackay and K. M. Ralls

December 1966

EFFECTS OF LOW-TEMPERATURE AGING ON THE RESISTIVE TRANSITION OF SUPERCONDUCTING 70Zr-30Nb (Cb) IN PULSED MAGNETIC FIELDS

M. Suenaga, J.L. O'Brien*, V.F. Zackay and K.M. Ralls

Inorganic Materials Research Division, Lawrence Radiation Laboratory,
Department of Mineral Technology, College of Engineering
University of California, Berkeley, California

December 1966

ABSTRACT

The effects of aging at 400°C on the resistive transition at 4.2°K of a superconducting 70Zr-30Nb alloy are reported. Microstructural changes were studied by critical temperature, resistive critical field, residual resistivity and microhardness measurements and by x-ray diffraction, optical microscopy and replication electron microscopy. The result of the aging treatment is a fine array of ω-phase particles with a mean center to center interparticle spacing of about 800Å. At an aging time of 300 hr. the maximum onset critical current density is reached. The particle size at the maximum current density is about 420Å. At times longer than 300 hr. effective particle impingement leads to lower onset critical current densities.

* A.D. Little, Inc., Cambridge, Mass.

INTRODUCTION

A defect-free Type II superconductor in a magnetic field above H_{c1} cannot sustain a transport current perpendicular to the applied field without power loss in the sample.[1-3] This power loss is due to flux line motion caused by the Lorentz force and is manifested by a longitudinal voltage.[4-6] When defects are present in the material, flux lines are pinned until the Lorentz force exceeds the "pinning force". That is, it is thought that flux lines reside in free-energy wells existing at the defects, and the critical Lorentz force is that which when integrated over distance will supply the free-energy difference necessary to move the flux line into a defect-free region of the superconductor.[7,8] Critical current density measurements obtained from the onset of longitudinal voltage for a given magnetic field and temperature provide an indirect measure of the critical Lorentz force or the pinning strength of the defects.

Various theoretical problems involving flux line motion and pinning have been investigated. Intrinsic resistance to flux line motion or "viscosity" has received some attention.[9-11] Flux line pinning due to defects and the effect of defect spacing, extent and type have received less consideration.[12] The qualitative relation between pinning strength and the microstructural defects involved is becoming well-established by experimental studies.[13-17] This is particularly true in magnetization experiments where specific defects have been shown to have definite effects.[18-20] The inherent difficulty with magnetization experiments is due to the unknown magnetic induction and macroscopic current distributions. A definite relationship between critical current density as a function of magnetic field and defect structure cannot be readily established. Even in direct critical current density vs field studies the development

of a quantitative relationship between microstructure and critical current density has been hampered because competing effects (e.g., cold work and precipitation) have been involved. Also, metallographic analysis of specimens has proven difficult, especially for high-field materials. With this in mind we have undertaken a study of a 70Zr-30Nb solid-solution alloy which is known to produce a very fine array of ω-phase particles on low-temperature aging. Well-annealed alloy strip was chosen as starting material so that the effect of this single process could be studied. Parallel determinations of superconductive properties and of microstructure are reported here.

EXPERIMENTAL PROCEDURE AND RESULTS

A. Material Preparation

The alloy (70Zr-30Nb) was made in a cold-mold arc furnace under a gettered inert gas atmosphere and was homogenized for 2 hr. at 920°C in high vacuum. After having been cold rolled to a 6-mil (0.015 cm) thickness, the alloy was sealed in an evacuated quartz capsule ($< 10^{-6}$ Torr), recrystallized and further homogenized in the single-phase bcc region of the phase diagram at 920°C for 2 hrs. Following a water quench portions of the alloy were aged at 400°C for various times in evacuated quartz capsules in order to precipitate the ω-phase. Specimens were 1 cm long with approximately 0.015 cm by 0.051 cm cross sections.

B. Property Measurements

Specimen ends were ultrasonically tinned with indium and then soft-soldered to the copper current connectors of a specimen holder. Voltage connections were made by pressure contacts approximately 0.45 cm apart. Specimens were inserted into a liquid helium dewar which was surrounded by a pulsed magnetic field coil (rise time: approximately 8 msec). Critical magnetic field and critical current density as a function of transverse

magnetic field were determined at 4.2°K. The procedure involved pulsing the magnetic field while maintaining a constant current in the specimen. The voltage across the specimen and the current through a previously calibrated pulsed-field coil were displayed simultaneously on a dual beam oscilloscope and were recorded with high-speed Polaroid film. Thus, for various current density levels both the beginning (J_{cS}) and the end (J_{cN}) of the superconducting transition as well as the change of voltage with magnetic field were observed.

Representative changes of the critical current density of the alloy for several aging times are shown in Fig. 1a, b, c and d. These correspond to aging treatments at 400°C of 0 (unaged), 10, 300 and 600 hours, respectively. J_{cS} designates the first appearance of voltage and J_{cN}, the fully normal state as the magnetic field is increased. The small insets in Fig. 1 show schematically the variation of specimen voltage with time for various constant values of applied current density as well as the pulsed-field coil current as a function of time. Minima in specimen voltage curves (Fig. 1a,b) indicate that the "peak effect" occurs for certain aging times. The critical magnetic field (Table I) is taken as that field which leads to completely normal behavior (H_{rN}) at low current densities (about 20A/cm^2).

The critical temperature shift (ΔT_c) in zero magnetic field of the aged specimens relative to the unaged specimen was determined with a calibrated, low-temperature germanium resistor. The transition was traced by a standard four-point resistive method with a search current density of less than 1 A/cm^2. Changes of the search current density by an order of magnitude in either direction resulted in negligible shifts of the transition curves. The variation of ΔT_c with aging time is shown in Table I.

C. Metallurgical Studies

Microstructural changes were studied by X-ray diffraction, optical microscopy, diamond pyramid microhardness determinations, residual electrical resistivity measurements, and carbon replication electron microscopy. Electron beam microprobe analysis indicated compositional homogeneity for all aging treatments, at least on the scale of the incident electron beam ($\geq 1\mu$ in diameter).

X-ray diffraction studies were made with nickel-filtered copper $K\alpha$ radiation in a scanning diffractometer. All specimens displayed strong bcc lines; the lattice parameter for the unaged specimen, obtained by extrapolation to $\theta = \frac{\pi}{2}$, is $a_o = 3.500 \pm 0.001\text{Å}$, which is in good agreement with published values.[21] No definite change in bcc phase lattice parameters with aging time was discernible. Peak broadening at the longer aging times, presumably due to strains resulting from the fine-scale precipitation, limited the accuracy of the bcc lattice parameter determinations to two decimal places. Specimens aged 100 hr. or less exhibited bcc β-phase peaks only; those aged 300 hr. or more exhibited hexagonal ω-phase peaks as well as β-phase peaks. The approximate lattice parameters of the ω-phase as determined from low-angle diffraction peaks are $c \approx 3.12\text{Å}$, $a \approx 5.03\text{Å}$ and $c/a \approx 0.620$, in reasonable agreement with published values.[22] Within the accuracy of two decimal places, no change in these values was noted for aging times of 300 to 1000 hrs. Diffraction lines of the hcp α-phase were not observed with any specimen.

Optical microscopy indicated a clean, single-phase structure for the unaged material. Aging of a recrystallized specimen for 1 hr. resulted in no detectable change. Treatments for 10 hr. and longer caused a very fine-scale precipitation with precipitate-free (nude) regions near the grain

boundaries and dense precipitate particle populations in the interiors of the grains. As aging time increased, the size of the nude regions near the grain boundaries decreased (Fig. 2a,b,c).

Diamond pyramid microhardness (DPH) determinations on metallographically prepared specimens indicated an increasing hardness with aging time (Fig. 3). The most significant increase occurs between 100 and 300 hrs. The shape of the microhardness curve is similar to others for zirconium-rich Zr-Nb alloys.[23] Residual (normal) electrical resistivity (Fig. 3) varies with aging time in an inverse manner to microhardness. This apparently reflects a lower residual resistivity of the ω-phase and, perhaps, partial zirconium depletion of the β-phase. Microhardness and residual resistivity seem to indicate a continuation of the precipitation process with increasing aging time, a fact which was not apparent from optical microscopy alone. Thus an effort was made to determine the size and distribution of precipitate particles as a function of aging time.

It was intended that transmission electron microscopy be employed to resolve this problem. Unfortunately, the non-uniform response of the specimens to chemical or electrolytic polishing prevented the preparation of suitable thin sections. Preparation of carbon replicas of electrolytically polished and etched surfaces proved somewhat more successful, and the structures for the 100, 300 and 600 hr. aging treatments were delineated, although only that for 300 hrs. could be seen quite clearly. The regular array of the precipitate particles after 300 hrs. of aging is striking (Fig. 5a,b). For 100 hrs. the average interparticle, center to center spacing is about 810Å and the average particle diameter is less than 330Å. For 300 and 600 hrs. the average interparticle spacings are about 800 and 790Å, respectively, and the average particle diameters are

about 420 and 480Å, respectively. Thus, the particle spacing remains almost constant, but the size of the particles increases with aging time.

DISCUSSION

Of the superconductive properties studied only critical current density varies strongly with aging treatment. Within the accuracy of the determination, critical field (H_{rN}) remains constant (Table I). The onset critical field (H_{rS}), however, is slightly decreased at the longest aging times (Fig. 1d). This may be indicative of zirconium-depletion in the matrix β-phase surrounding the ω-phase particles. In support of this interpretation is the observation that critical temperature is increased for the two longest aging times (Table I).[24]

Onset critical current density is known to be sensitive to metallurgical structure.[13-17] As shown in Fig. 1a,b,c, and d, J_{cS} increases rapidly for the shorter aging times (10 hrs. or less), while the end of the transition (J_{cN}) remains almost invariant. For the longer aging times J_{cS} and J_{cN} have the same trend, both passing through a maximum at 300 hrs. The rapid rise and fall of J_{cS} is accompanied, however, by lesser relative changes in J_{cN}. The cause of the variation of J_{cN} is uncertain. On the other hand, the variation of J_{cS} can be understood in terms of flux line pinning.[4-7]

Variation of the Lorentz force pinning parameter, $\alpha = |B \times J_{cS}| \doteq J_{cS}H$, with aging time is shown in Fig. 4. It is apparent that for aging times between 100 and 600 hrs. a significant enhancement of flux line pinning results, relative to that for the unaged material. The maximum value of α found in this study is about 1.68×10^5 kG · A/cm^2 for 300 hrs. at 400°C. This result suggests that for a single precipitation process there must be an optimum precipitate particle size which will lead to a maximum J_{cS}.

An understanding of the microstructure is necessary for explaining the observed superconductive properties. Therefore, a brief discussion of the possible solid-state transformations follows. Limited data exist on the athermal $\beta \rightarrow \omega+\beta$ transformation temperature as a function of composition for Zr-Nb alloys.[22] An extrapolation of these data to 30% niobium indicates that a 70Zr-30Nb alloy should not undergo the diffusionless transformation even down to liquid helium temperature. Hence, preexisting nuclei will not be present prior to aging, and the materials studied will not suffer any structural changes between room temperature and 4.2°K. Nevertheless, because of the tendency to form a faulted structure and because of the simple crystallographic relationship between the β- and ω-structures, it is likely that the interphase surface energy barrier to nucleation will be small. This appears to be substantiated by the fine-scale, apparently homogeneous nucleation which is responsible for the precipitate arrays shown in Figs. 2 and 5.

In a study of an 85Zr-15Nb alloy[25] it was shown that the β+ω faulting which resulted from quenching did not lead to a high onset critical current density, but subsequent isothermal aging at 400°C did. Likewise, in the work reported here the results must be interpreted in terms of the precipitation and growth which occur as aging time increases. Two primary effects are noted: first, the particles in the interiors of the grains grow, and second, the nude regions next to the grain boundaries decrease in extent. At first sight, the latter might be used to explain the behavior of J_{cS} as a function of aging time: the regions of low resistance to flux line motion are decreased in size as aging time increases. No doubt this has some importance, but it would not indicate the decrease in α realized at the longest aging times employed. It is more likely that the size of the

ω-phase particles in the grain interiors has primary importance, since this rather than their center to center spacing is what changes with aging time. A comparison of particle size and spacing with the computed area per flux line at several magnetic fields is given in Table II. This data suggests that a distribution of particles each having an area about two to four times that of a flux line and occupying (in the aggregate) about 20% of a cross-section provide effective pinning. The geometrical distribution of particles is probably important also, but is fixed here. Because the particles are arrayed in a regular manner, but not uniformly (Fig. 5), it is likely that for very long aging times they effectively impinge upon one another along rows and thus provide channels for easy flux line motion. This is the most plausible explanation for the behavior of the specimens aged for 600 and 1000 hr. Optical metallography indicated no significant structural change for these specimens relative to the one aged for 300 hr. However, surface replicas of the 600 hr specimen viewed with an electron microscope tended to support the idea that rows of ω-phase particles effectively impinge.

Pinning models which utilize barriers either independent of magnetic field or decreasing in the same manner as the free energy difference between the normal and mixed states lead to a considerably more rapid decrease in J_{cS} with H than is found for the specimen aged 300 hr. That is, the slow decrease in J_{cS} with H (Fig. 1c) is indicative of a pinning barrier which increases slightly as H increases, as would be expected if local composition gradients are produced. Either the effective number of pinning sites increases with field or the effective size of existing pinning sites increases with field. At the longest aging times, where impingement of the ω particles decreases their effectiveness in pinning, composition gradients

are spread over longer distances, thus decreasing their effectiveness.

CONCLUSIONS

Isothermal aging at low temperature provides a useful way to study the effect of a single precipitation process on the flux line pinning strength of high-field superconductive alloys. It is found that, for a constant ω-phase particle dispersion in the interiors of grains of a 70Zr-30Nb alloy, the onset critical current density increases as ω-phase particle size increases until effective impingement of the ω particles occurs. At the same time that ω-phase particles are growing, the extent of the nude regions next to grain boundaries decreases in size due to the onset of precipitation in the regions continguous to the precipitate areas. This additional precipitation presumably contributes to the observed increase in J_{cS}, as well. Negligible changes in H_{rN} indicate that no gross composition changes occur in the matrix, yet slight changes in H_{rS} and in T_c may correspond to zirconium-depletion of the matrix region around ω-phase particles. The composition gradients thus set up probably add to the pinning strength exhibited by the alloy.

Because of the composition gradients and the effective particle impingement at very long aging times, a quantitative relationship between pinning strength and microstructure could not be obtained. An experiment to obtain such a relationship must involve a material for which composition gradients are minimized and not only particle size but also particle distribution can be varied. Such an investigation is currently under way.

ACKNOWLEDGMENTS

The authors wish to thank Dr. Kurt Kennedy for assistance with the experimental phase of this work, Dr. Robert G. Boyd for helpful discussions, Mr. Georges Brun for performing the electron microscopy, Mr. Donald Wixson for performing the optical metallography, and Professor Marshal F. Merriam for critically reading the manuscript.

This work was supported under the United States Atomic Energy Commission through the Inorganic Materials Research Division of the Lawrence Radiation Laboratory.

Table I. Critical temperature shift (ΔT_c) and resistive critical field (H_{cN}) of aged 70Zr-30Nb.

Aging time (hr)	ΔT_c(°K)	H_{cN}(kG)
Unaged	—	89
1	-0.1	85
10	0	84
100	-0.2	84
200	—	86
300	0	87
600	+0.6	88
1000	+0.9	86

Table II Flux line areas and ω-phase particle sizes

H(kG)	Area per flux line* $\frac{\Phi_o}{H}$ (μ^2)
20	10×10^{-4}
30	6.67×10^{-4}
40	5×10^{-4}
50	4×10^{-4}
60	3.33×10^{-4}

* $\Phi_o \simeq 2\times10^{-7}$ G cm^2, the flux quantum

Aging time (hr)	Average total area per particle (μ^2)	Average area of an ω particle $\frac{\pi}{4} d^2$(μ^2)	Area fraction occupied by ω particles (%)
100	6.5×10^{-3}	($<8.6\times10^{-4}$)	(<13)
300	6.4×10^{-3}	13.9×10^{-4}	22
600	6.3×10^{-3}	18.1×10^{-4}	29

REFERENCES

1. C. J. Gorter: Phys. Letters, 1962, vol. 1, pp. 69-70.

2. R. A. Kamper: Phys. Letters, 1963, vol. 5, pp. 9-10.

3. W. Klose: Phys. Letters, 1964, vol. 8, p. 12.

4. P. W. Anderson and Y. B. Kim: Rev. Mod. Phys., 1964, vol. 36, pp. 39-43.

5. Y. B. Kim, C. F. Hempstead, and A. R. Strnad: Rev. Mod. Phys., 1964, vol. 36, pp. 43-45.

6. Y. B. Kim, C. F. Hempstead, and A. R. Strnad: Phys. Rev., 1965, vol. 139, pp. A1163-72

7. Y. B. Kim, C. F. Hempstead, and A. R. Strnad: Phys. Rev., 1963, vol. 131, pp. 2486-95.

8. J. D. Livingston and H. W. Schadler: Progr. Mat. Sci., 1964, vol. 12, no. 3.

9. M. Tinkham: Phys. Rev. Letters, 1964, vol. 13, pp. 804-07.

10. M. J. Stephen and J. Bardeen: Phys. Rev. Letters, 1965, vol. 14, pp. 112-13.

11. P. Nozieres and W. F. Vinen: Phil. Mag., 1966, vol. 14, pp. 667-88.

12. J. Friedel, P. G. De Gennes, and J. Matricon: Appl. Phys. Letters, 1963, vol. 2, pp. 119-21.

13. J. B. Vetrano and R. W. Boom: J. Appl. Phys., 1965, vol. 36, pp. 1179-80.

14. D. Kramer and C. G. Rhodes: Trans. Met. Soc. AIME, 1965, vol. 233, pp. 192-98.

15. H. B. Shukovsky, K. M. Ralls, and R. M. Rose: Trans. Met. Soc. AIME, 1965, vol. 233, pp. 1825-32.

16. F. W. Reuter, K. M. Ralls, and J. Wulff: Trans. Met. Soc. AIME, 1966, vol. 236, pp. 1143-51.

17. D. A. Colling, K. M. Ralls, and J. Wulff: Trans. Met. Soc. AIME, 1966, vol. 236, pp. 1218-23.

18. J. D. Livingston: Rev. Mod. Phys., 1964, vol. 36, pp. 54-57.

19. T. H. Alden and J. D. Livingston: Appl. Phys. Letters, 1966, vol. 8, pp. 6-7.

20. J. D. Livingston: Appl. Phys. Letters, 1966, vol. 8, pp. 319-20.

21. B. A. Rogers and D. F. Atkins: Trans. AIME, 1955, vol. 203, pp. 1034-41.

22. D. J. Cometto, G. L. Houze, Jr., and R. F. Hehemann: Trans. Met. Soc. AIME, 1965, vol. 233, pp. 30-39.

23. B. A. Hatt and J. A. Roberts: Fulmer Research Institute Report, R114, Jan. 5, 1959.

24. J. K. Hulm and R. D. Blaugher: Phys. Rev., 1961, vol. 123, pp. 1569-80.

25. A. H. King, J. L. O'Brien, J. A. Roberts, and P. R. Roberts: Cryogenics, 1965, vol. 5, pp. 230-31.

FIGURE CAPTIONS

Fig. 1 The critical current densities, J_{cS} and J_{cN} vs magnetic field, H, and the resistive transition behavior with magnetic fields for constant current densities. (a) The unaged specimen, as-quenched from 920°C, (b) the specimen aged for 10 hr at 400°C, (c) the specimen aged for 300 hr at 400°C, and (d) the specimen aged for 600 hr at 400°C.

Fig. 2 Optical micrographs of 70Zr-30Nb alloy quenched from 920°C, and (a) aged for 100 hr at 400°C, (b) aged for 300 hr at 400°C, and (c) aged for 600 hr at 400°C. 2000×

Fig. 3 The variation of diamond pyramid microhardness (DPH) for 100 gm load and of residual resistivity, ρ, at 4.2°K with aging time.

Fig. 4 The variation of the Lorentz-force parameter, α, at H = 40 kG with aging time.

Fig. 5 Carbon replication micrographs of 70Zr-30Nb alloy quenched from 920°C and aged for 300 hr at 400°C. a) 12,000×, and b) 48,000×.

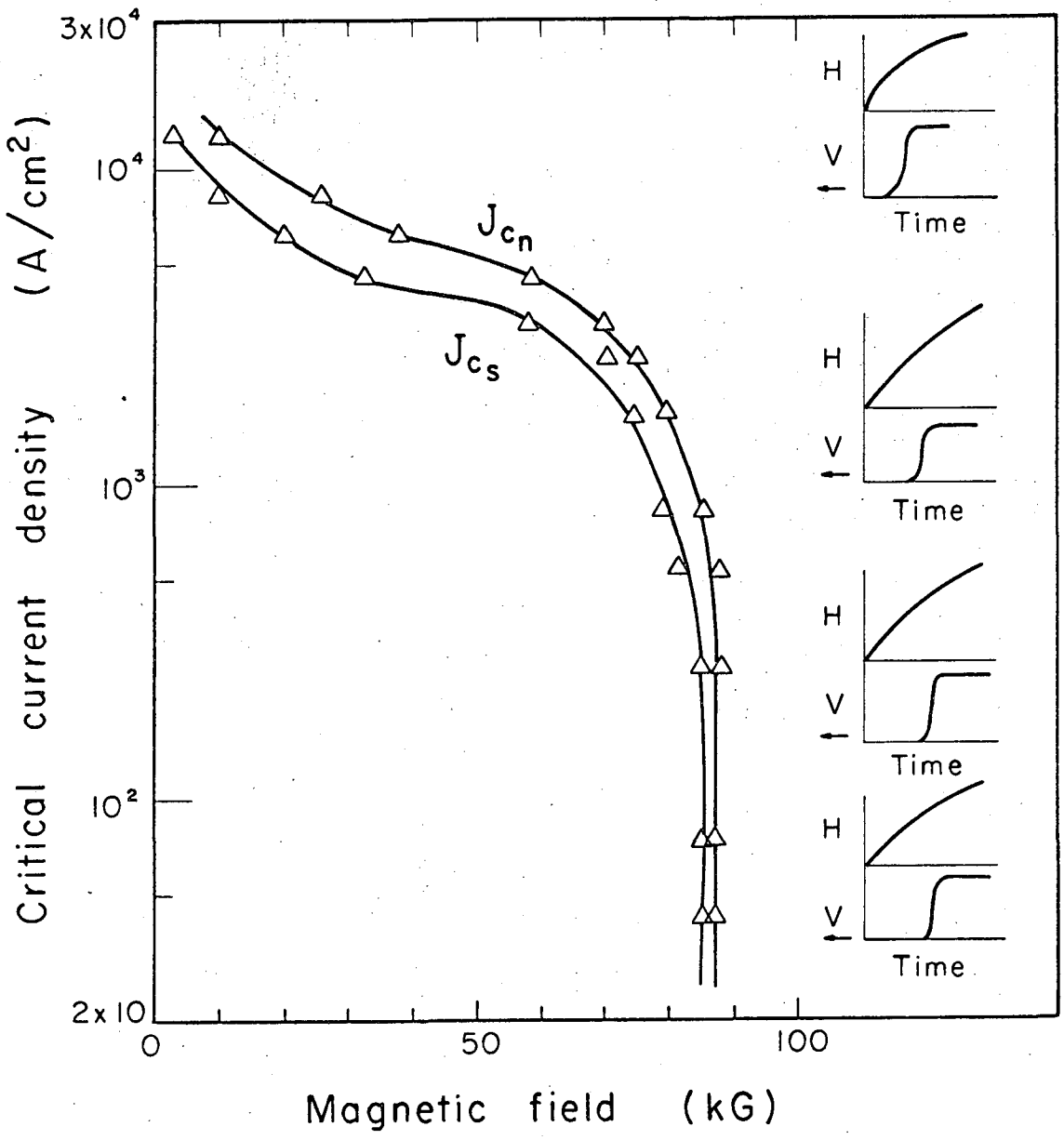

MUB-8927

Fig. 1c

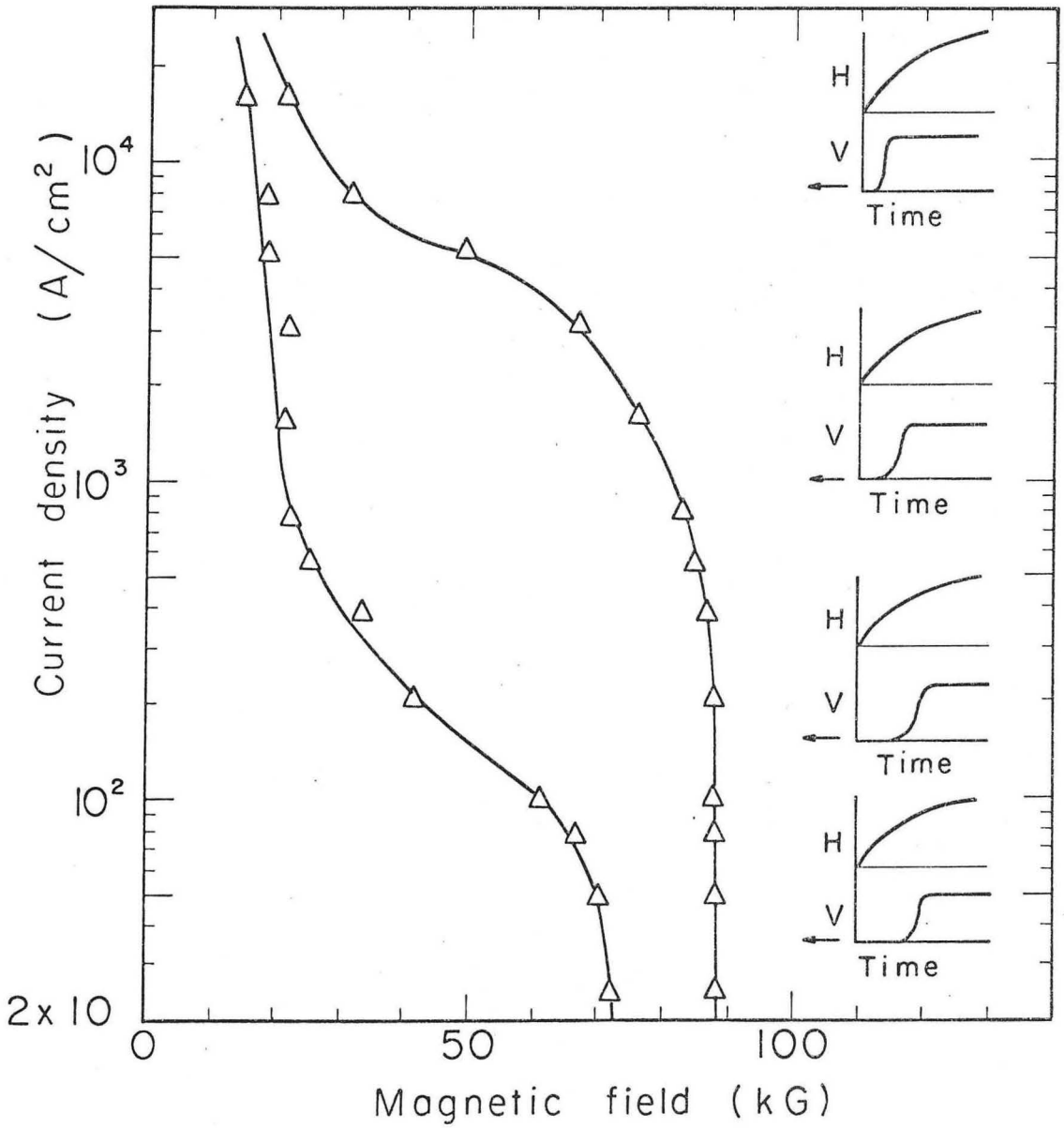

MUB-13863

Fig. 1d

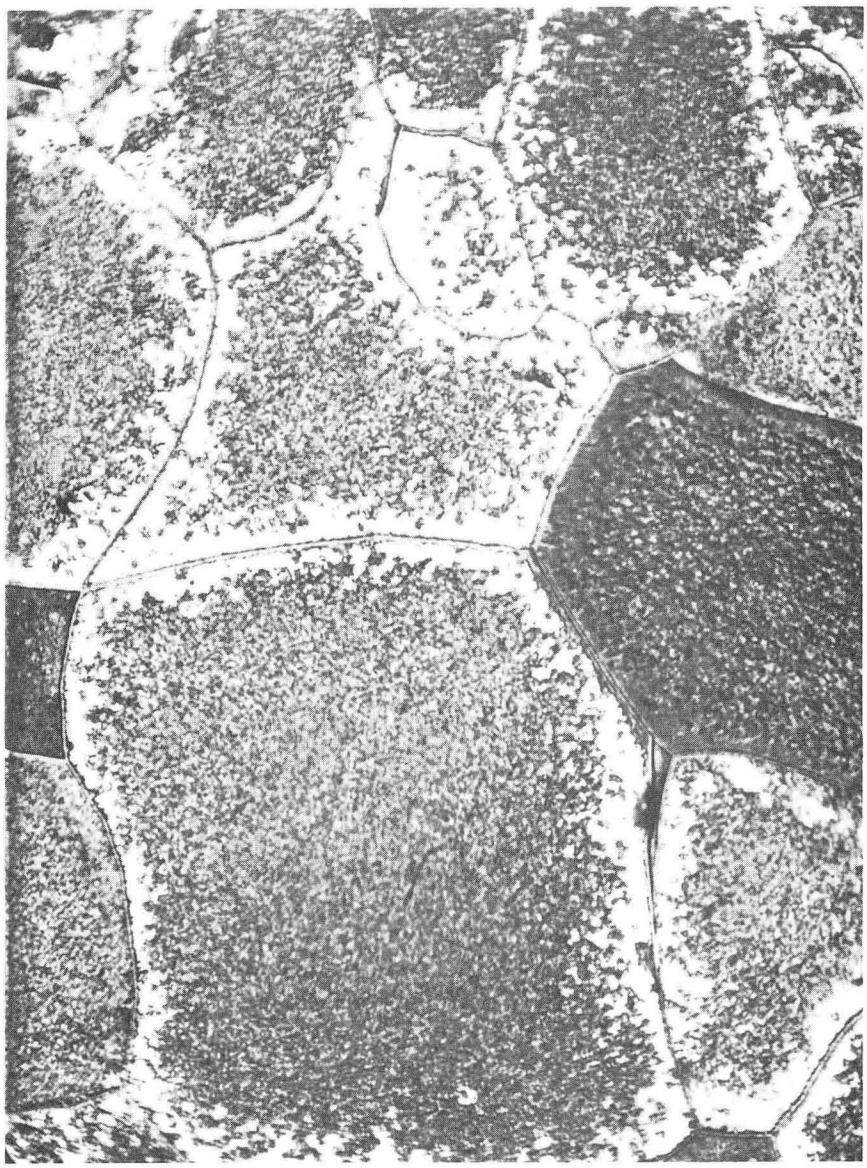

BBH 672-22

Fig. 2a

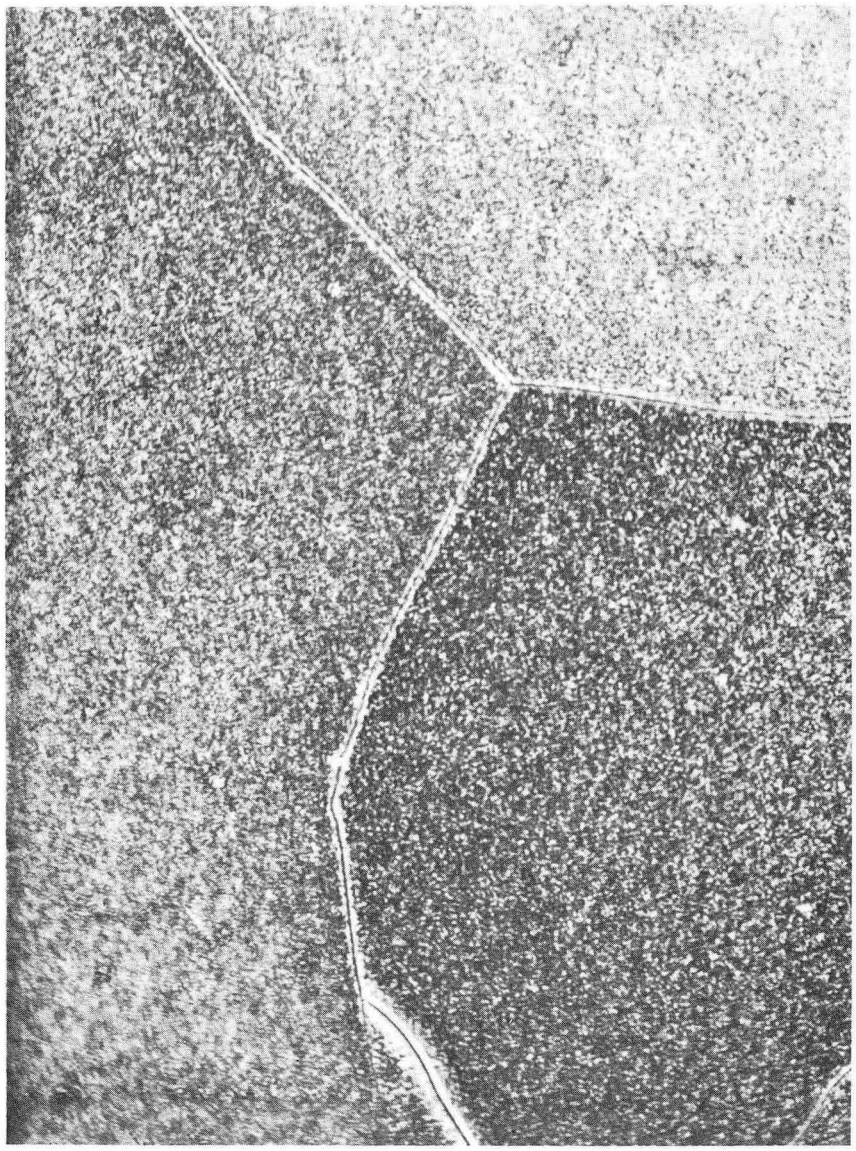

BBH 672-23

Fig. 2b

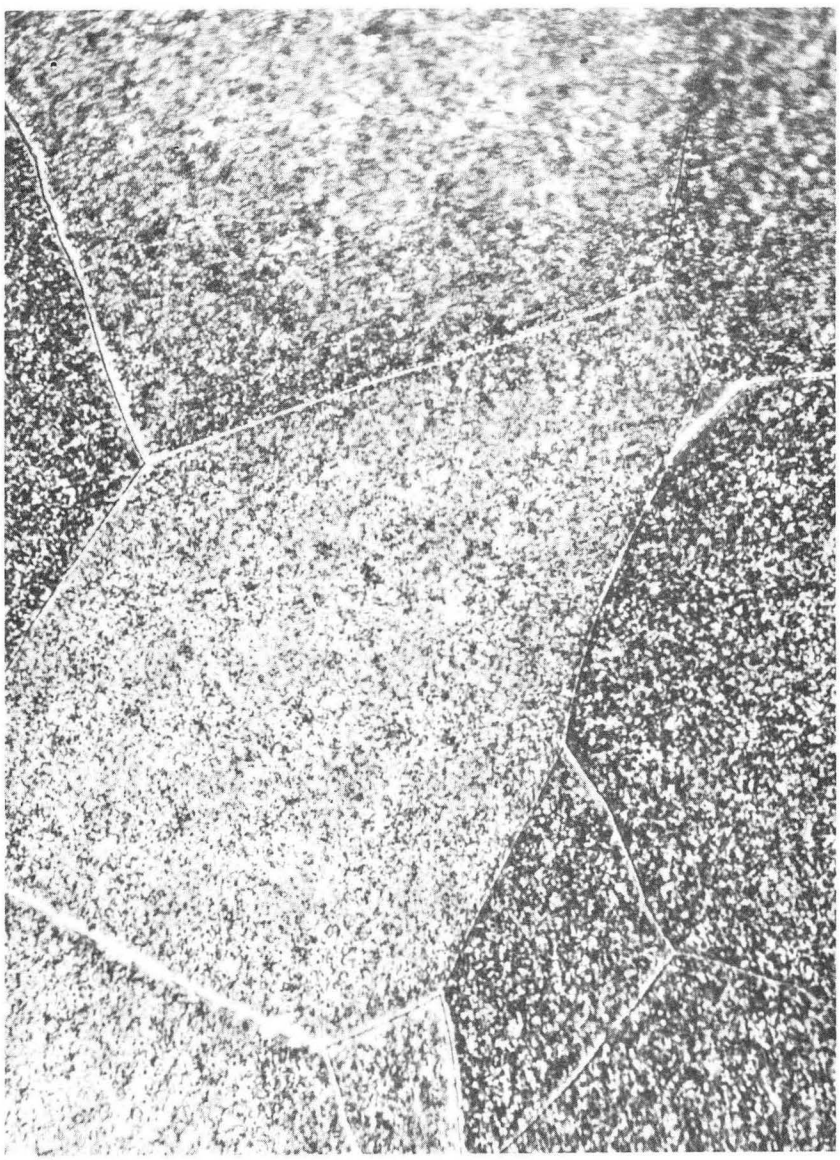

BBH 672-24

Fig. 2c

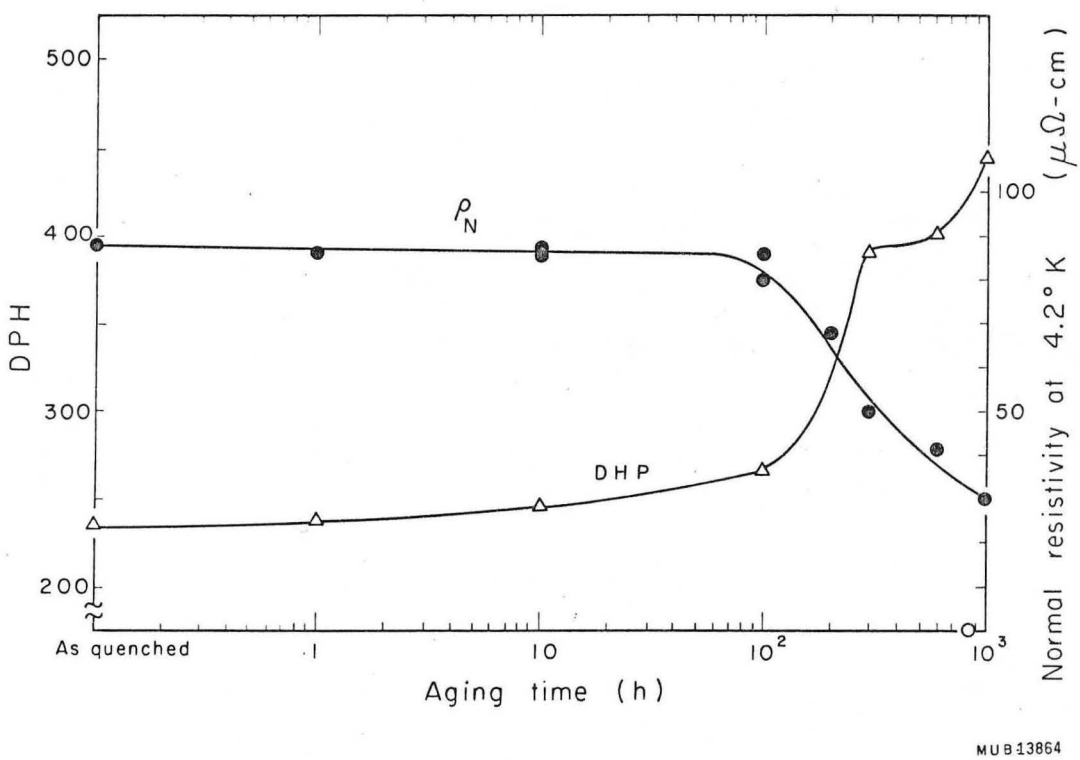
500
400
300
200
DPH
ρ_N
DHP
100
50
Normal resistivity at 4.2° K ($\mu\Omega$-cm)
As quenched
.1
10
10^2
10^3
Aging time (h)
MUB 13864

Fig. 3

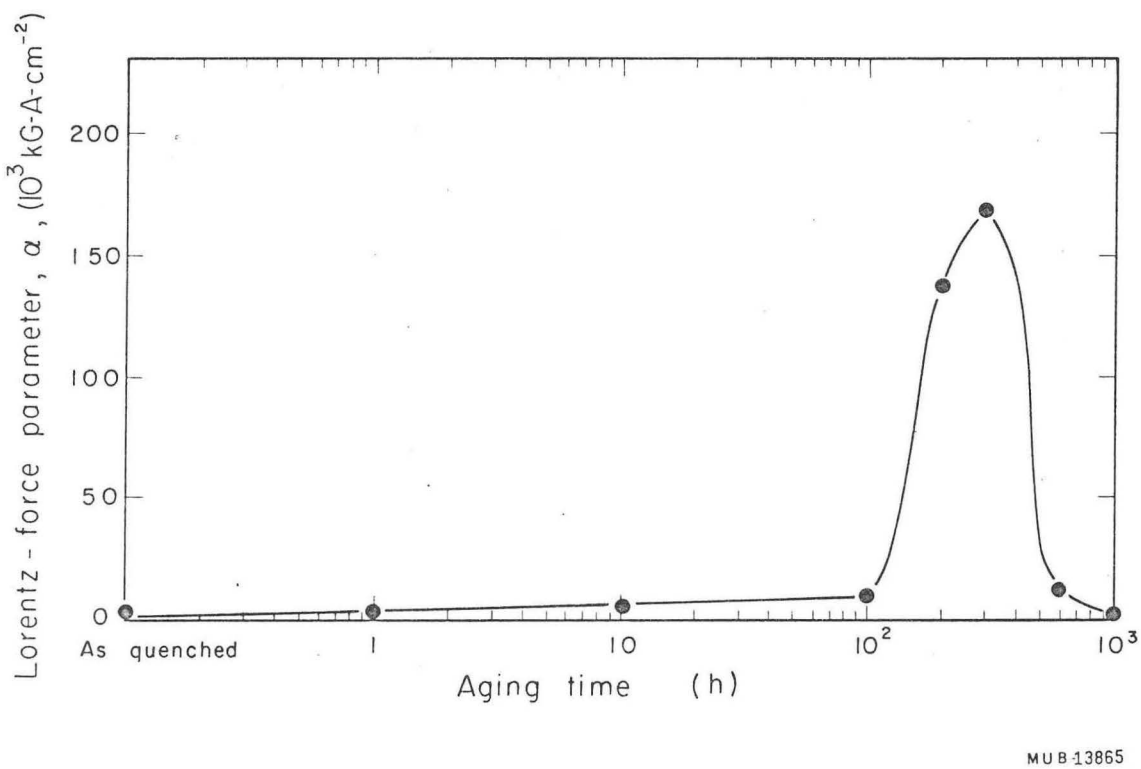
Lorentz - force parameter, α, (10³ kG-A-cm⁻²)
200
150
100
50
0
As quenched
1
10
10²
10³
Aging time (h)
MUB-13865

Fig. 4

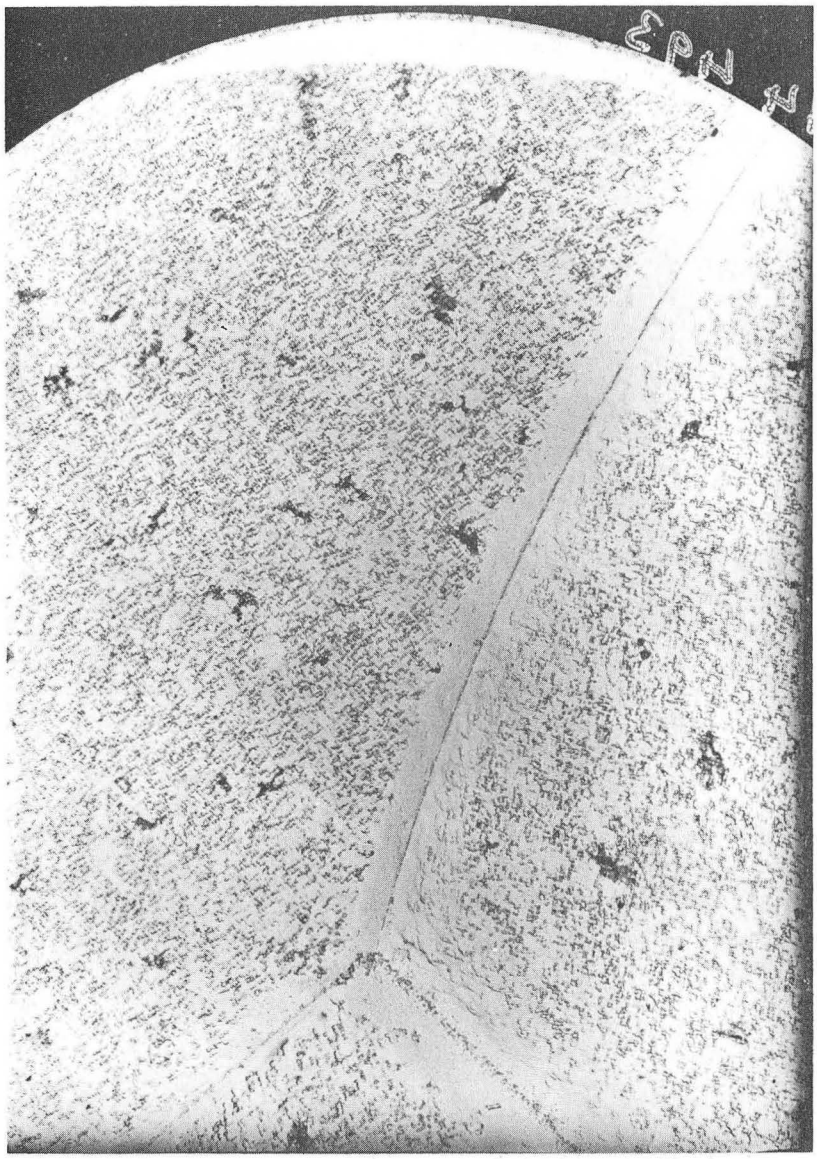

BBH 672-25

Fig. 5a

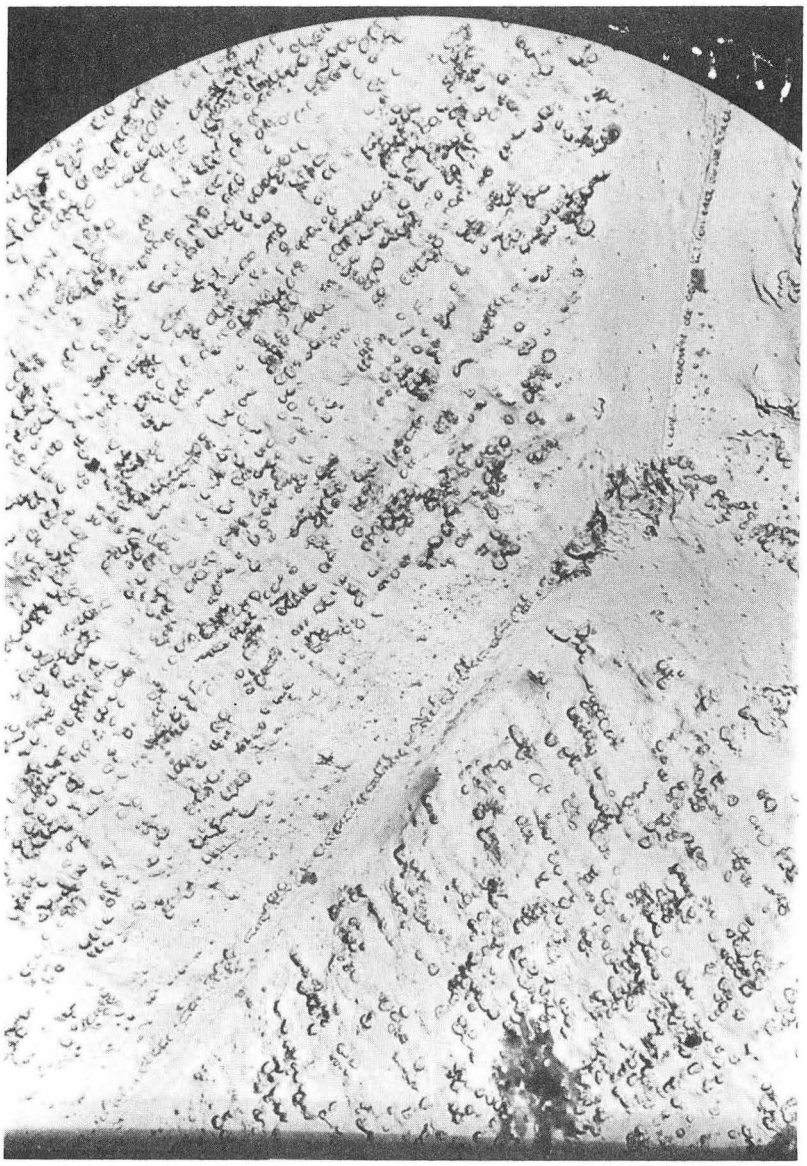

BBH 672-26

Fig. 5b

This report was prepared as an account of Government sponsored work. Neither the United States, nor the Commission, nor any person acting on behalf of the Commission:

A. Makes any warranty or representation, expressed or implied, with respect to the accuracy, completeness, or usefulness of the information contained in this report, or that the use of any information, apparatus, method, or process disclosed in this report may not infringe privately owned rights; or

B. Assumes any liabilities with respect to the use of, or for damages resulting from the use of any information, apparatus, method, or process disclosed in this report.

As used in the above, "person acting on behalf of the Commission" includes any employee or contractor of the Commission, or employee of such contractor, to the extent that such employee or contractor of the Commission, or employee of such contractor prepares, disseminates, or provides access to, any information pursuant to his employment or contract with the Commission, or his employment with such contractor.